Stereodynamics of ring and nitrogen inversion in spiroheterocycles. Conformational analysis of *N*-methylspiro[morpholine-3,2′-adamantane] and *N*-methylspiro[piperidine-2,2′-adamantane] using NMR spectroscopy and theoretical calculations

Antonios Kolocouris,† Emmanuel Mikros * and Nicolas Kolocouris

Division of Pharmaceutical Chemistry, Department of Pharmacy, University of Athens, Panepistimiopolis, 15 771 Zografou, Greece

Adamantane forces the *N*-methyl group of *N*-methylspiro[morpholine-3,2′-adamantane] 1 and *N*-methylspiro[piperidine-2,2′-adamantane] 2 to adopt an axial orientation and to undergo a slow enantiomerization as depicted by dynamic ^{1}H and ^{13}C NMR spectroscopy. The observed enantiomerization freezes below 0 °C as evidenced by the fully resolved protons and carbons of adamantane in NMR spectra. The observed resonances are interpreted using 2D NMR spectroscopy. Interconversion between the two enantiomeric forms is demonstrated by exchange spectroscopy (EXSY). The activation energy at the coalescence point is calculated from the ^{13}C NMR spectra and found to be 14.3 and 15.2 kcal mol^{-1} for molecules 1 and 2, respectively. Theoretical calculations suggest a mechanism of interconversion where the significant transition state is the one separating two twist-boat forms.

Introduction

The conformational behaviour of various alicyclic tertiary amines has attracted special consideration, partly because of their occurrence in many complex natural and synthetic molecules of pharmacological interest.[1] Stereoelectronic factors that affect the rate of inversion and rotation in different classes of amines have been reported.[2] Elegant studies have been recently reported on multicyclic amines where nitrogen inversion is significantly restricted.[3]

In *N*-alkyl heterocyclic amines, like piperidine and morpholine, interconversion between conformational isomers involves nitrogen and ring inversion processes. The significant transition state for ring chair–chair reversal is the one separating the boat family forms from the chair. It is generally considered that the lowest energy path from the chair to the twist-boat proceeds *via* a half chair conformation in which four ring atoms are coplanar (C_2 symmetry).[1b] Other forms have also been considered as a possible transition state for six-membered ring inversion[4] suggesting a fluxional transition state for chair to twist-boat interconversion. The kinetic parameters for these processes were affected by suitable substitution, however, in all reported cases, interconversion is fast (on the NMR timescale) at room temperature.[1b,c]

N-Methylspiro[morpholine-3,2′-adamantane] **1**, *N*-methylspiro[piperidine-2,2′-adamantane] **2** and related systems are at least equipotent to the drugs amantadine and rimantadine against the influenza A virus (H1N1, H2N2, H3N2)[5] and exhibit activity against HIV-1 that is worth investigating.[6] The

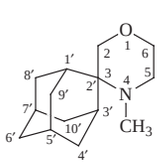

1

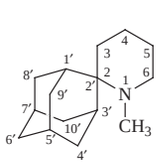

2

† Present address: National Research Foundation, Institute of Organic and Pharmaceutical Chemistry, Vasileos Constantinou 48, Athens 11635, Greece.

^{1}H NMR spectra of compounds **1** and **2** at room temperature present structureless and broadened resonances suggesting an unusually slow conformational interconversion.

Scheme 1 depicts the conformational changes of six-membered heterocycles.[1a–c] It is apparent that in compounds **1** and **2** the interchangeable ChAx-ChAx′ conformers, where the *N*-methyl group adopts an axial position, are enantiomers and the same is true for ChEq-ChEq′ where the *N*-methyl group adopts an equatorial position. The interconversion of enantiomeric conformations ChAx-ChAx′ or ChEq-ChEq′ may proceed *via* a pathway which involves either ring inversion followed by nitrogen inversion or nitrogen inversion followed by ring inversion. The interconversion presented in Scheme 1 is

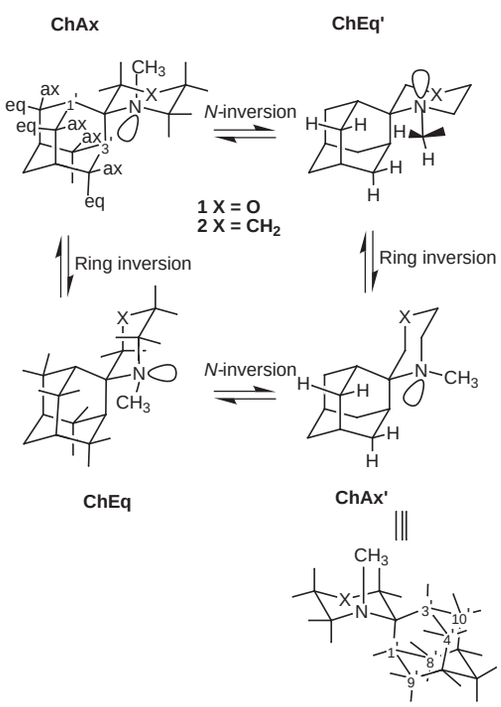

Scheme 1

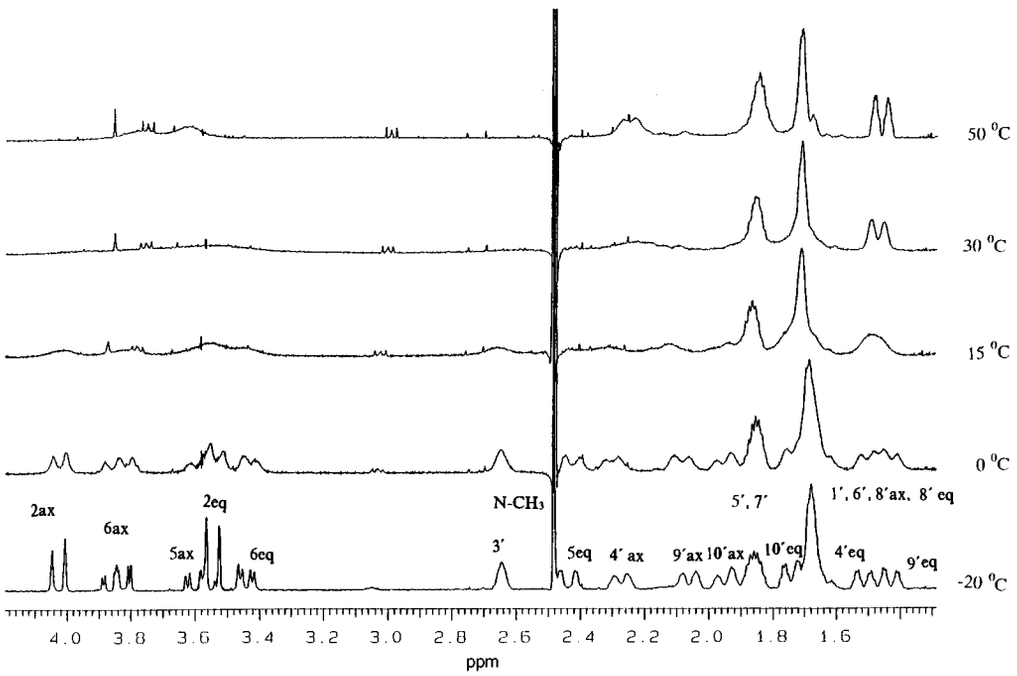

Fig. 1 Variable temperature ^{1}H NMR spectra (250 MHz) of *N*-methylspiro[morpholine-3,2′-adamantane] **1**

expected to be slowed down because of the spirostructure rigidity and the bulk of the adamantane moiety. This slow interconversion is not observed for the parent *N*-H amines in a wide range of temperatures, suggesting that the presence of the *N*-methyl substituent in **1** and **2** results in an effective interaction with the adamantyl nucleus.

In the present study, the stereodynamics of the conformational interconversions of spiromorpholine **1** and spiropiperidine **2** have been examined by means of dynamic NMR spectroscopy, exchange spectroscopy[7] and theoretical calculations. These interesting polycyclic amines undergo a slow enantiomerization, on the NMR timescale, at room temperature. At low temperatures the ^{1}H and ^{13}C NMR spectra are relatively well resolved. The conformational preferences around the nitrogen of heterocycles **1** and **2** at low temperatures make all carbon and hydrogen nuclei of adamantane diastereotopic, giving rise to separate signals in the NMR spectra. An unequivocal assignment of the observed peaks has been performed using 2D homonuclear and heteronuclear correlation spectra. The NMR spectra of adamantane derivatives[8–10] have been extensively studied since the rigid structure of the adamantane nucleus can be used as a model to explore SCS (substituent chemical shifts). It is notable that although the analysis of the ^{13}C NMR spectra of different 2,2-disubstituted adamantanes has been reported,[10] only a few data have been published on their ^{1}H NMR spectra. Exchange spectroscopy clearly demonstrated that an equilibrium exists between two enantiomeric species and theoretical calculations are in agreement with the spectral data which show an axially oriented predominant conformation for the *N*-methyl substituent. Molecular mechanics calculations were also undertaken in order to clarify the energetics of conformational changes. All possible transitions between different low energy conformers are described and an interconversion pathway between ChAx to ChAx′ is proposed.

Results and discussion

NMR spectra

Spiromorpholine 1. The 250 MHz ^{1}H NMR spectrum of the morpholine derivative **1** has been recorded at different temperatures ranging from +50 to −50 °C. In the range of +50 to 0 °C the spectral lines are broad (Fig. 1). At +50 °C the resolution is enhanced but still this temperature is well below the fast exchange limit. At temperatures lower than 0 °C the spectrum remains unchanged and displays resolved signals (Fig. 1) which can be analysed (Table 1).

The assignment of the resonances of the morpholine moiety at these temperatures is straightforward as all the signals are shifted downfield and they do not interfere with the adamantane signals. At low temperatures, where the interconversion is slow in the NMR timescale, only one set of morpholine signals is observed. This points out the existence of two conformational enantiomers in the equilibrium. As shown in Scheme 1, the interconversion between the enantiomers permutes the morpholine geminal protons 2ax-2eq, 5ax-5eq, 6ax-6eq, and the adamantane protons 1′-3′, 4′ax-9′ax, 4′eq-9′eq, 8′ax-10′ax and 8′eq-10′eq. Thus, in order to prove this enantiomerization, the phase sensitive NOESY (EXSY) spectrum at −20 °C (300 MHz) has been recorded (Fig. 2). In this spectrum cross peaks arising from exchange phenomena have the same phase as the diagonal, while NOE cross peaks indicating spatial proximity have opposite phase to the diagonal. It is clear in Fig. 2 that exchange cross peaks exist between the 2ax and 2eq, 5ax and 5eq, 6ax and 6eq protons of the morpholine moiety as well as between the 4′ax and 9′ax, 4′eq and 9′eq, 1′ and 3′ protons of the adamantane nucleus (cross peaks correlating 8′ and 10′ protons are not as clear because of overlapping).

Molecular mechanics calculations on enantiomeric conformations ChEq and ChEq′ where the *N*-methyl group adopts an equatorial position revealed that they encountered severe steric interactions with the adamantane skeleton. Thus, the relative energies of ChEq and ChEq′ are ~9 kcal mol^{-1} higher than for enantiomeric conformations ChAx and ChAx′ where the *N*-methyl group is axial. These results suggest that the *N*-methyl heterocycle favours enantiomeric conformations ChAx and ChAx′.

The above mentioned steric phenomena slow down the conformational interconversion and thus the coalescence point for the exchange between ChAx and ChAx′ is observed at about 30 °C (250 MHz). When no substituent is present on the morpholine nitrogen, interconversion is fast and no change is visible in the NMR spectrum down to −50 °C (250 MHz). It is also interesting to note that in *N*-methyl-3,3-dimethylmorpholine the ring inversion process freezes below −80 °C while the nitrogen inversion process freezes at a much lower temperature.[11]

Table 1 ^{1}H and ^{13}C NMR chemical shifts and coupling constants for *N*-methylspiro[morpholine-3,2′-adamantane] **1** and *N*-methylspiro[piperidine-2,2′-adamantane] **2** (−20 °C, 250 MHz)

	N-Methylspiro[morpholine-3,2′-adamantane]			*N*-Methylspiro[piperidine-2,2′-adamantane]		
Atoms	δ_H	*J*/Hz	δ_C	δ_H	*J*/Hz	δ_C
2ax	4.02	12.4	63.1			60.0
2eq	3.54	12.4				
3ax			57.5	1.85		22.2
3eq				1.33		
4ax				1.75		19.3
4eq				1.55		
5ax	3.56	14.7, 11.4, 3.9	47.7	1.68	11.8	18.2
5eq	2.44	14.7		1.14		
6ax	3.84	12.0, 11.4, 2.4	60.0	3.19	13.7, 3.1	47.6
6eq	3.44	12.0, 3.9		2.58	13.7	
1′	1.64		31.0	1.60		34.5
2′			57.5			57.9
3′	2.64		28.4	2.43		28.7
4′ax	2.26	12.7	31.3	2.40	12.5	31.4
4′eq	1.51	12.7, 2.5		1.44	12.5	
5′	1.85		27.2[a]	1.80		27.2[a]
6′	1.66		38.3	1.65		38.6
7′	1.85		26.9[a]	1.80		27.0[a]
8′ax	1.68		32.8	1.83		33.0
8′eq	1.63			1.58		
9′ax	2.06	12.3	31.5	2.20	12.5	31.7
9′eq	1.43	12.3, 2.6		1.40	12.5	
10′ax	1.95	13.1	33.1	1.84		33.0
10′eq	1.73	13.1, 2.7		1.64		
N-CH_3	2.48		33.6	2.36		34.0

[a] Chemical shifts of 5′ and 7′ carbons may be interchanged.

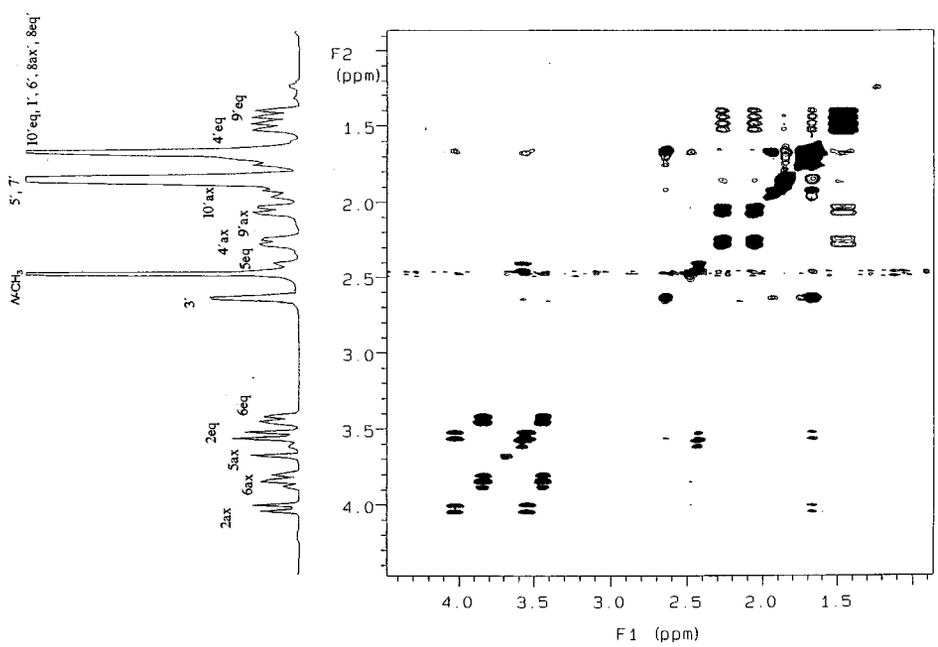

Fig. 2 Phase sensitive NOESY spectrum (300 MHz) of *N*-methylspiro[morpholine-3,2′-adamantane] **1** at −20 °C. Black coloured cross peaks, having the same phase as the diagonal, are due to exchange phenomena. The other cross peaks are due to NOE correlations.

Thus the presence of the adamantane framework hinders sterically the movement of the *N*-methyl group.

The assignment of the resonances of the adamantane moiety is more difficult due to serious overlapping between signals which are not well resolved as a result of their long range spin–spin couplings. A spectrum interpretation can be achieved on the basis of the COSY, the phase sensitive NOESY and the C–H correlation spectra recorded at −20 °C.

The ^{1}H NMR spectra of 2,2-disubstituted adamantane derivatives reported in the literature exhibited the following eight different kinds of protons: (a) 1,3-H (b) 4ax,9ax-H (c) 4eq,9eq-H (d) 5-H (e) 6-H (f) 7-H (g) 8ax,10ax-H (h) 8eq,10eq-H.[12] Van Deursen and Korver analysed the ^{1}H NMR spectra of OH, Cl, Br, I and NH_2 2-substituted adamantanes.[8b] The most characteristic feature of these spectra is the AX pattern of geminal 4′ax-4′eq and 9′ax-9′eq protons. This results in a downfield doublet of the chemically equivalent 4′ax and 9′ax protons, because of their 1,3-*syn*-axial position with respect to the 2-heterosubstituent, and an upfield doublet of the corresponding 4′eq and 9′eq protons. *N*-Methylmorpholine **1**, can be regarded as a 2,2-disubstituted adamantane. At −20 °C, where interconversion processes are frozen, the different adamantane protons are diastereotopic, and 13 different resonance signals are present in the ^{1}H NMR spectrum of **1**. From this spectrum,

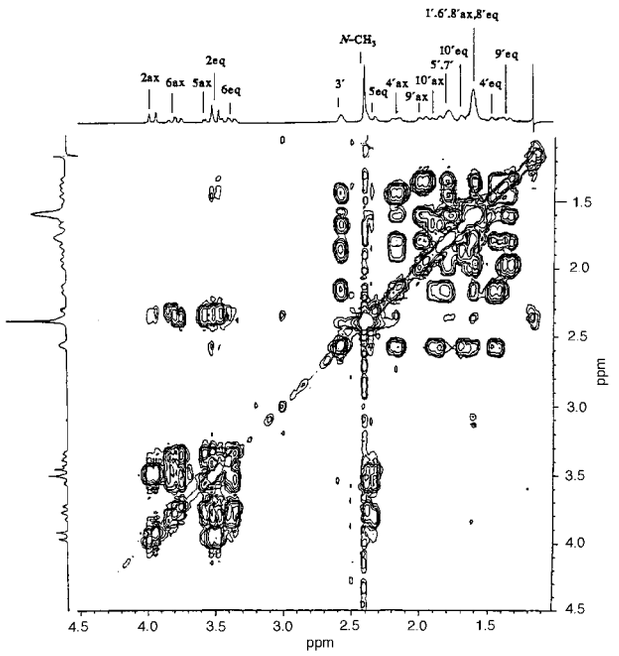

Fig. 3 COSY spectrum (250 MHz) of *N*-methylspiro[morpholine-3,2′-adamantane] **1** at −20 °C

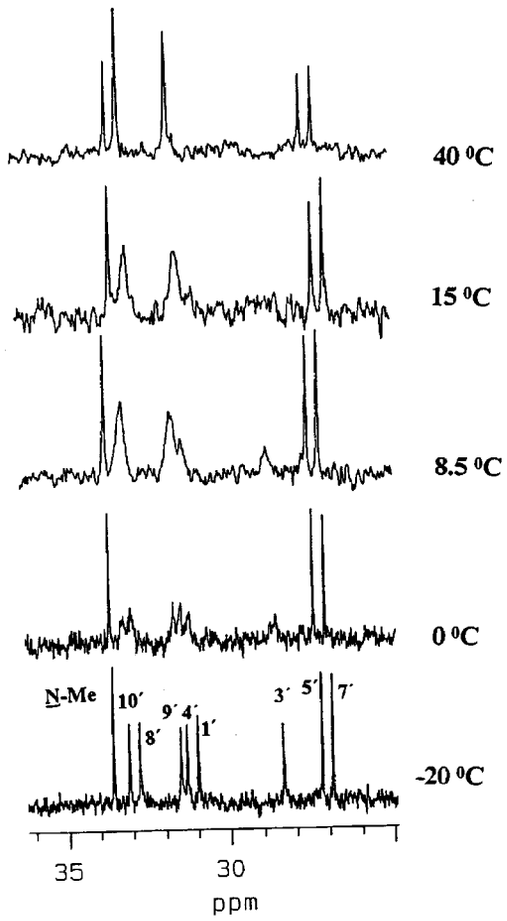

Fig. 4 Variable temperature ^{13}C NMR spectra (300 MHz) of *N*-methylspiro[morpholine-3,2′-adamantane] **1**

the doublets of the geminal adamantane protons (AX pattern) can easily be recognized.

The ^{13}C–^{1}H correlation spectrum allows the distinction of several overlapping proton signals and especially signals corresponding to the bridge (4′,9′ and 8′,10′—the corresponding carbons show correlations with two different protons) and bridgehead (1′,3′ and 5′,7′) protons of adamantane. The phase sensitive NOESY spectrum can also distinguish the pairs of protons in exchange from peaks of protons correlated through space (Fig. 2).

The NOESY spectrum allows the assignment of proton 1′ at 1.64 ppm because it exhibits space proximity with the 2ax and 2eq morpholine protons and with *N*-methyl at 2.48 ppm. This proton is in exchange with the broad singlet at 2.64 ppm assigned to proton 3′. In the COSY spectrum proton 3′ correlates with four other protons which ought to be 4′ax, 4′eq, 10′ax and 10′eq (Fig. 3). Among them the more deshielded at 2.26 ppm is assigned to 4′ax because it is in a 1,3-diaxial position with respect to the morpholine nitrogen. The 4′ax proton is in exchange with 9′ax at 2.06 ppm and shows an intense spin coupling with the resonance at 1.51 ppm assigned to 4′eq. The 9′ax proton has an intense scalar correlation with the doublet at 1.43 ppm and is assigned to 9′eq. The 10′ax proton is assigned at 1.95 ppm as it exhibits a strong COSY correlation with 3′ and a weak 'W' coupling with 4′ax. The strong COSY correlation of 3′ at 1.73 ppm is attributed to the 10′eq proton. The 4′ and 9′ protons correlate strongly with the resonance at 1.85 ppm attributed to proton 5′ and 4′ax correlates weakly with the resonance at 1.66 ppm assigned to the 6′ proton. The 10′ax proton is in exchange with proton 8′ax assigned at 1.68 ppm and overlapping with 8′eq at 1.63 ppm as depicted in the ^{13}C–^{1}H correlation spectrum. The 7′ proton overlapping with 5′ can be assigned from the ^{13}C–^{1}H correlation spectrum at 1.85 ppm. The observed signal shapes of bridge (broad doublets) and bridgehead (broad singlets) adamantane protons as well as the coupling constant values (J_{gem} ~ 12 Hz, J_{vic} ~ 3 Hz) are as expected[8] (Table 1).

The 75.5 MHz ^{13}C NMR spectrum of the morpholine derivative **1** at −20 °C is interpreted on the basis of the ^{13}C–^{1}H correlation spectra and DEPT experiments (Table 1).

The axial orientation preference of *N*-methyl is supported by the observed downfield shift of protons 2ax, 5ax and 6ax relative to the corresponding equatorial protons (Fig. 1). This can be attributed to the effect exerted by the β-antiperiplanar axial *N*-methyl group on the 6ax proton[13] and the steric interaction of the protons of the methyl group with the *syn*-axial ring protons 2ax and 5ax ('steric shift'[13b]). In addition, some ^{13}C NMR data show good agreement with an axial structure. Thus, the observed resonance of *N*-methyl carbon at 33.6 ppm indicates an axial orientation.[1c,14] The upfield shifts of carbons 2 (−10 ppm), 6 (−8 ppm) and 1′ (−5 ppm), with respect to the corresponding carbons of the parent *N*-H heterocycle, are also attributed to the γ-*gauche* effect[14,15] of the axial *N*-methyl group.[16]

The ^{13}C NMR spectrum showed also a temperature dependence (Fig. 4). As expected, no spectral changes were observed for morpholine ring and *N*-methyl carbons. The variable temperature NMR study showed changes only for adamantane carbons. At low temperatures (−20 °C) carbons 8′, 10′ show two distinct signals. The same is observed for carbons 4′, 9′ and 1′, 3′. At slow exchange temperatures all adamantane carbons are diastereotopic and consequently give separate signals. There are only few examples in the literature[9j] of such resolution in 2,2-disubstituted adamantanes. The observed resonances of the adamantane as well as morpholine carbons are supported from literature data obtained from derivative compounds.[1c,8b,14] Thus, the resonances of 4′ and 9′ carbons were observed at higher fields relative to those of 8′ and 10′ carbons. Carbon 3′ is shifted 2.6 ppm upfield relative to carbon 1′. Carbon 3′ resonance is expected to bear two γ-*gauche* upfield steric shifts from morpholine oxygen and C-5 and a weak β-deshielding effect from the anti-periplanar *N*-methyl. Carbon 1′ resonance bears a γ-*gauche* upfield shift from axial *N*-methyl and a weak γ-*anti* upfield shift[9g,15] from morpholine oxygen.

Table 2 Comparison of equilibrium free energy differences (up) and *N*-inversion barriers (down) for some piperidine heterocycles as calculated by semi-empirical methods and molecular mechanics

	Exp	AM1	PM3	MM+	MM2*	MM3*
Compound	ΔG_0[a]/kcal mol^{-1}	ΔE_0[a]/kcal mol^{-1}				
N-H Piperidine	0.4	−2.8	−2.3	0.1	0.3	0.3
N-Methylpiperidine	2.7	−1.2	−1.4	2.1	2.6	2.0
1,2,2,6-Tetramethylpiperidine	1.9	−0.6	−0.7	1.6	1.7	1.6
	$\Delta G^{\ddagger}$[b]/kcal mol^{-1}	$\Delta E^{\ddagger}$[b]/kcal mol^{-1}				
N-H Piperidine	6.1	6.8	10.0	4.8	4.3	4.8
N-Methylpiperidine	8.7	5.1	7.7	9.5	8.9	4.9
1,2,2,6-Tetramethylpiperidine	11.0	4.8	8.9	8.7	8.2	8.7
2-Methyl-2-azabicyclo[2.2.2]octane	6.6	5.6	8.3	4.7	3.8	4.2

[a] ΔG_0 and ΔE_0 are the experimental and calculated energy difference between the chair conformations with axial and equatorial orientation of the substituent at the nitrogen atom. [b] $\Delta G^{\ddagger}$ and $\Delta E^{\ddagger}$ are the experimental and calculated values respectively of the *N*-inversion barrier.

At a higher temperature (~0 °C, 75.5 MHz) the two signals corresponding to 8′ and 10′ carbons or 4′ and 9′ carbons coalesce to a single line at 36.1 and 33.0 ppm respectively, because of the increased rate of exchange between the enantiomeric conformations ChAx and ChAx′. The free energy of activation ($\Delta G^{\ddagger}$) is calculated using the coalescence temperature (278 ± 4 K) and the frequency difference of the carbons 4′ and 9′ at −20 °C. This is found to be 14.3 ± 0.2 kcal mol^{-1}.[17]

Spiropiperidine 2. From the combined ^{1}H, ^{13}C NMR data and molecular mechanics calculations the axial preference of the *N*-methyl group is also established in piperidine **2**. The ^{1}H and ^{13}C NMR spectra of *N*-methylspiro[piperidine-2,2′-adamantane] **2** exhibit an analogous temperature dependence as the morpholine derivative **1**. The 250 MHz ^{1}H NMR spectrum is broad in the range between 10 and 50 °C. The analysis of the spectra at −20 °C has also been performed by combining COSY, the ^{13}C–^{1}H correlation and 2D phase sensitive NOESY spectra and data are presented in Table 1. The ^{1}H NMR spectrum of compound **2** exhibits extended overlapping between the adamantane and the piperidine resonances resulting in a complex and less resolved spectrum.

^{13}C NMR spectra were obtained in the same temperature range. The coalescence temperature for the 4′ and 9′ carbon resonances is at 305 ± 4 K (75.5 MHz) and the energy of activation ($\Delta G^{\ddagger}$) calculated for this temperature was found to be 15.2 ± 0.2 kcal mol^{-1}.

Ring inversion barriers already reported[1c] for *N*-methylmorpholine and *N*-methylpiperidine are 11.5 (−31 °C) and 11.0 (−28 °C) kcal mol^{-1} respectively. The energy barriers for the ChAx to ChAx′ interconversion for the spiro *N*-methylmorpholine **1** (14.3 kcal mol^{-1}) and the spiro *N*-methylpiperidine **2** (15.2 kcal mol^{-1}) are significantly higher as expected from the experimental observation that the process is slow in the NMR timescale at room temperature. It also worth noting that the energy barrier for ring inversion in *N*-methylmorpholine is higher than that for *N*-methylpiperidine ring inversion, while the opposite trend is observed for spiroheterocycles **1** and **2**.

Theoretical calculations

Theoretical calculations were combined with NMR spectroscopy in order to obtain a detailed conformational analysis. Compounds **1** and **2** are of too high molecular weight to be subjected to high-level *ab initio* calculations with full geometry optimisation; on the other hand, as will be discussed below, empirical force field molecular mechanics calculations (like MM2 calculations) have not been parametrized for the planar nitrogen configuration in order to describe the nitrogen inversion. We hoped therefore that semiempirical MO calculations might prove useful for our molecules. In order to test their efficiency in molecules with structures relative to **1** and **2**, we applied semiempirical methods AM1 and PM3 to compare between calculated and experimental ground state and *N*-inversion barrier energies for *N*-H piperidine,[1c] *N*-methylpiperidine,[1c] 1,2,2,6-tetramethylpiperidine[18] and 2-methyl-2-azabicyclo[2.2.2]octane.[3a] However the experimental results are not in good agreement with calculated ones, as can be seen in Table 2. In contradiction with experiment,[1c,3a,18] AM1 and PM3 calculations place the conformer where the nitrogen methyl is axial as the global minimum and clearly underestimate the energy barrier of *N*-inversion. A similar failure of semiempirical AM1 and PM3 calculations to predict global minima correctly in nitrogen heterocyclic systems has been reported by other authors.[19] The energy values calculated using the three different MM force fields (MM2*, MM3*, MM+) were in good agreement with experimental data in describing the ground states of axial and equatorial structures (Table 2). The *N*-inversion barrier has been calculated, using molecular mechanics, by setting the molecular geometry to constrain the nitrogen and three attached carbons to the same plane. MM2* and MM+ do not give results consistent with experimental data as they are not parametrized for *N*-inversion, and seem to underestimate the *N*-inversion barrier (Table 2).

Considering the failure of semi-empirical methods to predict the energies for minima and transition states in the former nitrogen heterocycles we were imposed to use only molecular mechanics calculations for compounds **1** and **2** under study, which predict correctly the relative energies of the minima. For comparison reasons, the *N*-inversion barrier was calculated using MM as an approximate estimation, as has already be done by Forsyth *et al.*,[3a] knowing that energies will be probably underestimated.

The conformational space for molecules **1** and **2** was initially explored by applying a Monte Carlo search using the MM2* force field.[20a] The geometries of the different ground state conformers and their energies are summarised in Table 3. In the piperidine derivative **2** six different twist-boat structures corresponding to local energy minima were found (TW1, TW2, TW3, TW4, TW5, TW6) as well as the chair with *N*-methyl in the axial orientation, ChAx, and the chair with *N*-methyl in the equatorial orientation, ChEq. In the morpholine derivative **1** only the first four of the corresponding twist-boat structures were found, along with ChAx and ChEq forms.

To describe the possible interconversion pathway we calculated the transition state energies for the conversion of each twist-boat (TWi) to the axial, equatorial and the neighbour twist-boat conformations (TWi ± 1) using the MM+ force field[20b] and the following procedure. Starting from each twist-boat conformation we varied two torsion angles of the heterocyclic ring in steps of 10° over the angular range corresponding to each particular conformational interconversion, keeping a third torsion angle under constraint. For each conformational interconversion an energy map was plotted and the transition state was defined. In most cases, a second energy map was calculated in a more restricted angle range around the transition

Table 3 Low energy conformers of morpholine **1** and piperidine **2**. Individual twist-boat conformers are denoted in terms of the location of the *N*-methyl substituent and the spiroadamantane nucleus relative to the heterocycle as isoclinal (I_c), pseudoaxial (ψ_a), and pseudoequatorial (ψ_e). Relative energies were calculated using the MM+ force field

			E_{rel}	
Geometry	Description	Conformer	Morpholine **1**	Piperidine **2**
Chair	Me-ax	ChAx	0	0
Twist-boat	Me(ψ_a), Ad(ψ_a, ψ_e)	TW1	4.3	6.8
Twist-boat	Me(I_c), Ad(ψ_a, ψ_e)	TW2	10.7	10.9
Twist-boat	Me(ψ_e), Ad[ψ_a, $\psi_e(g^+g^-)$]	TW3	13.9	16.1
Twist-boat	Me(ψ_e), Ad(ψ_a, ψ_e)	TW4	11.7	12.7
Twist-boat	Me(I_c), Ad[ψ_a, $\psi_e(g^+g^-)$]	TW5	*a*	17.1
Twist-boat	Me(ψ_a), Ad(I_c)	TW6	*a*	9.2
Chair	Me-eq	ChEq	8.4	9.4

[a] These conformers were not found for the morpholine derivative.

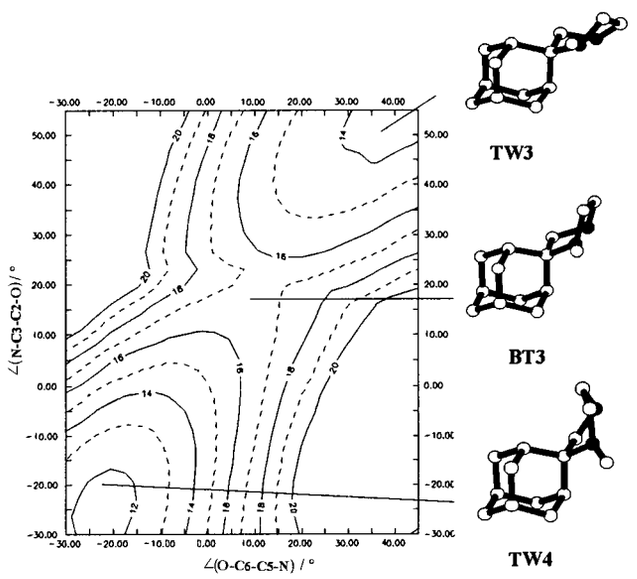

Fig. 5 Energy surface map for the interconversion of twist-boat TW3 to TW4 of morpholine **1**, as a function of C4–C5–C6–N and N–C2–C3–C4 angles. Isoenergy contours have been drawn for the range between 12–20 kcal mol^{-1} at 1 kcal mol^{-1} increments. The low energy conformations and the transition state have been represented. This map was realised by driving the C4–C5–C6–N angle from −30° (–24° in conformer TW4) to 40° (37° in conformer TW3) and the N–C2–C3–C4 angle from −30° (–24° in conformer TW4) to 55° (49° in conformer TW3), while C5-C6-N-C2 was constrained in the range between −44° to −67°.

state geometry, in steps of 2°. An example showing the energy map calculated for the TW3 to TW4 interconversion of molecule **1** is depicted in Fig. 5. The *N*-inversion barrier relating to each conformer was also calculated using the MM+ force field by constraining the nitrogen and three attached carbons to the same plane. The results of these calculations are summarised in Table 4.

From these calculations a possible pathway for interconversion of the morpholine **1** can be followed, as visualised in Fig. 6. In this sequence, a half-chair transition state (TS1) with C_2 geometry (four carbons coplanar) brings the ring into a twist-boat conformation (TW1). After three conversions between twist-boats (TW2, TW3 and TW4) the *N*-methyl group adopts a pseudo-equatorial position. Then, the chair conformation is again established through a new half-chair transition state (TS2). Finally, the *N*-methyl group is reoriented to the axial position *via* nitrogen inversion.

These calculations suggest that the energy barrier is not a transition state between a chair and a twisted boat, which usually is the case for six-membered rings,[1b,4] but a conformer close to a boat form (BT3), which connects the two twist-boat minima TW3 and TW4. In this structure, the *N*-methyl group is positioned in proximity to the adamantane nucleus (the distance between the methyl carbon and the 4′-H is 2.5 Å) resulting in a highly distorted CH_3–N–C2′ angle (121.2°). When theoretical calculations are compared with the experimental data they seem to overestimate the highest energy barrier but predict an energy of activation ($\Delta G^{\ddagger}$) difference of ~1 kcal mol^{-1} between the two derivatives found from the ^{13}C DNMR study.

It should be pointed out that other energetically favoured pathways involving nitrogen inversion directly from a twist-boat are possible. Moreover, the high energy transition state in the proposed pathway is structurally near to an *N*-inversion transition state having the nitrogen atom and the three attached carbons almost coplanar, suggesting that *N*-inversion can take place simultaneously during this step. The energy barrier calculated for the ChAx-ChAx′ interconversion is based on well parametrized equations. The less reliable calculation of the *N*-inversion has been taken into account only after the ring inversion process. However, for all possible ways for the *N*-inversion the main conclusion of this study should apply, namely, that the rate determining step involves a transition state which is not a half-chair conformation (usually seen in six-membered rings), and in which a severe g^+g^- interaction plays undoubtedly a very important role.

Comparing the two conformational energy maxima calculated for the morpholine **1** and piperidine **2** derivatives, the differences concerning the six-membered ring structure and the *N*-methyl group position are small. In the morpholine derivative **1** the distance between 1′-H and 6-H is longer (2.5 Å) than the corresponding 1′-H to 5-H distance (2.3 Å) in the piperidine derivative **2**. The distance between 8′-H and 2-H in **1** is again slightly longer (2.3 Å) than the corresponding 8′-H to 3-H in **2**. The major structural difference between the two transition states is the relatively short distance of 2.5 Å between the 4-H hydrogen of the piperidine moiety and the 3′-H of the adamantane in the BT3 transition state of derivative **2**. This steric interaction is not present in the BT3 transition state of derivative **1** and can probably explain the higher energy required for the interconversion in spiropiperidine **2**.

In conclusion, the steric interactions between the adamantane moiety and the *N*-methyl group result in a slow interconversion between enantiomeric ChAx and ChAx′ and, consequently, render diastereotopic all carbons and protons of the nitrogen heterocycle and the adamantane moiety. The unusually slow interconversion can be followed by DNMR and the energy of activation of the interconversion is found to be relatively high compared to parent heterocycles *N*-methylmorpholine and *N*-methylpiperidine. Theoretical calculations show that the rate determining step in the mechanistic pathway of interconversion is not a transition between a chair and a twisted boat as is usual for six-membered rings. This is attributed to the strong interaction between the *N*-methyl and adamantane hydrogens.

Table 4 Relative energies of the transition states for the interconversion between the different conformers of compounds **1** and **2** based on MM+ calculations. The values italicised show the lowest energy pathway for the interconversion between the two enantiomeric forms with the *N*-methyl group axial (ChAx-ChAx′)

		Transition state E_{rel}						
Compound	Comformer	TW1	TW2	TW3	TW4	TW5	TW6	ChAx
1	ChAx	*9.1* (TS1)	11.1		17.9			
	TW1						*a*	
	TW2	*11.1* (BT1)						
	TW3		*14.6* (BT2)					
	TW4			*16.3* (BT3)				
	TW5				*a*			
	TW6					*a*		
	ChEq	21.5	21.1	20.7	*14.7* (TS2)			
	N-Inversion	13.7	*b*	19.7	13.7			*10.4c* (TSN1)
2	ChAx	*8.8*	11.7	21.2	21.2	20.2	10.2	
	TW1						9.4	
	TW2	*11.3* (BT1)						
	TW3		*16.2* (BT2)					
	TW4			*17.8* (BT3)				
	TW5				21.9			
	TW6					17.2		
	ChEq	23.1	24.7	23.0	*15.2* (TS2)	22.6	23.7	
	N-Inversion	14.2	18.8	17.3	14.2	18.8	17.3	*10.3c* (TSN1)

[a] These transition states were not calculated as no local energy minima corresponding to TW5 and TW6 conformers were found for morpholine derivative **1**. [b] The *N*-inversion of TW2 should result in the enantiomeric form of TW5 but as TW5 was not found for the morpholine derivative **1** this transition state energy was not calculated. [c] *N*-Inversion transition state energy for ChAx-ChEq interconversion.

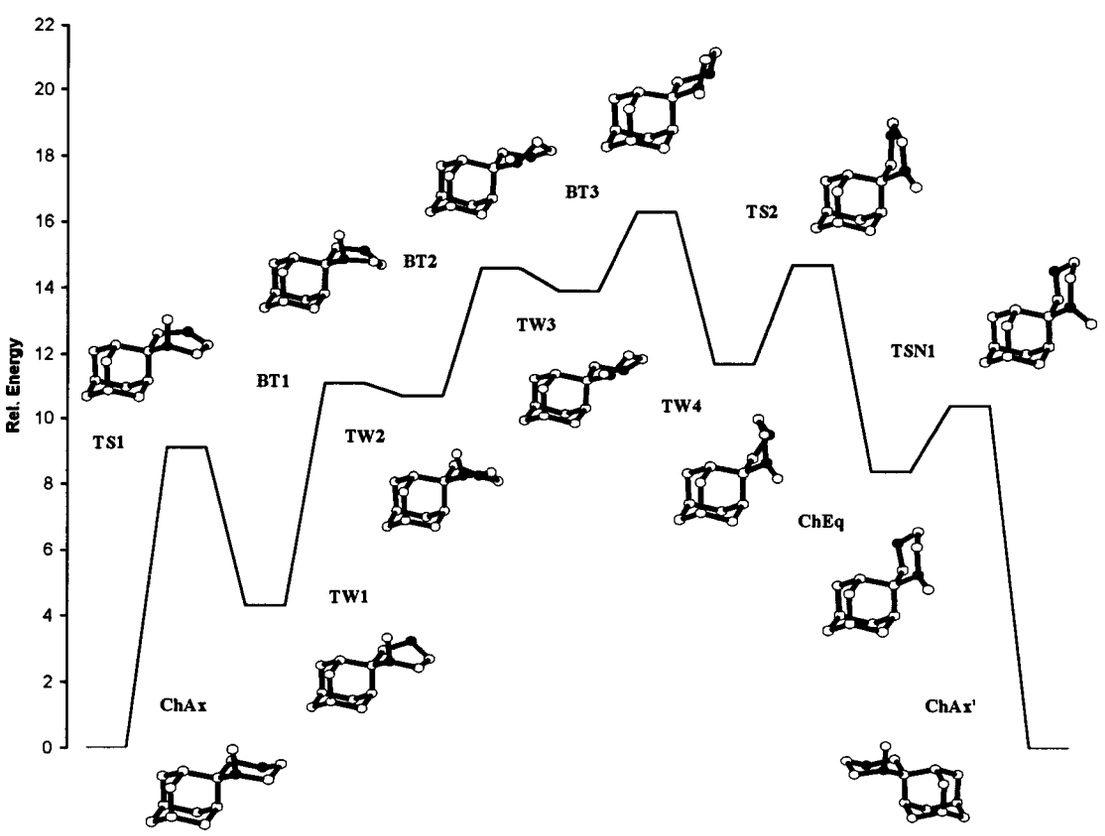

Fig. 6 Energy profile of the conformational changes of morpholine derivative **1** based on MM+ calculations

Experimental

NMR Spectroscopy

N-Methylspiro[morpholine-3,2′-adamantane] **1** and *N*-methylspiro[piperidine-2,2′-adamantane] **2** were prepared by methods described elsewhere.[5a] The NMR spectra were recorded on Bruker AC-250 MHz and Varian UNITYplus 300 MHz spectrometers in $CDCl_3$. The 2D experiments were carried out with the following parameters: (a) COSY spectral width 1200 Hz in both dimensions and four transients for each FID; 512 t_1 increments and recycling delay of 2 s; a sine weighting function was applied prior to Fourier transformation; (b) the phase sensitive NOESY was obtained with $t_m = 2.5$ s and a recycling delay of 2 s; spectral width 1100 Hz in both dimensions, 512 t_1 increments, a 512 × 512 data matrix and eight transients for each FID; a $\pi/2$ shifted sine-squared weighting function was applied prior to Fourier transformation; (c) the ^{13}C–^{1}H correlation spectra were obtained with 128 FIDs in the t_1 domain

and 1 K data points in the t_2 domain, eight transients for each t_1 increment and a recycling delay of 3 s; a $\pi/2$ shifted sine weighing function was applied prior to Fourier transformation.

Theoretical calculations

A conformational search was performed using the Monte Carlo method as incorporated in the Macromodel[20a] software on a Silicon Graphics Indy workstation (MM2*, 2000 steps, convergence criterion 0.05 kcal mol^{-1}). MM2* and MM3* force fields were used as implemented in Macromodel software. All other calculations were performed using the Hyperchem[20b] software on a Pentium PC. The force field used for molecular mechanics calculations was MM+ unless specially noted. The Polak–Ribiere (conjugate gradient) minimization method with an energy convergence criterion of 0.01 kcal mol^{-1} was used for geometry optimisation. Semi-empirical quantum mechanical methods AM1 and PM3 were used in combination with the RHF method and a convergence criterion of 0.01 kcal mol^{-1}, using the Polak–Ribiere (conjugate gradient) geometry optimisation method, was applied. The force constant applied to constrain the driven torsion angles for the calculation of the energy maps was 80 kcal mol^{-1} degree^{-2} for the driven torsion and the convergence criterion of 0.05 kcal mol^{-1}. A 16 kcal mol^{-1} degree^{-2} force was used for the third constrained torsion and 20 kcal mol^{-1} degree^{-2} for the nitrogen atom to keep the same stereochemistry. When the values of the two driven torsions that characterise the transition state were determined, the energy of the transition state was calculated after geometry optimisation with a convergence criterion of 0.01 kcal mol^{-1} without imposing the constraints for the third torsion and the nitrogen atom stereochemistry. A force constant of 160 kcal mol^{-1} degree^{-2} was applied for the calculation of the *N*-inversion transition states.

Cartesian coordinates of all low energy and transition state structures reported, for the different interconversions listed in Table 4 are available from Emmanuel Mikros (email: emikros@atlas.uoa.gr).

Acknowledgements

We would like to thank Professor J. Koca of the University of Brno and Dr T. Mavromoustakos of the Institute of Organic and Pharmaceutical Chemistry of National Hellenic Research Institute, Athens, for helpful discussions and Dr D. Argyropoulos of the University of Athens for technical assistance.

References

1 (*a*) I. D. Blackburne, A. R. Katritzky and Y. Takeuchi, *Acc. Chem. Res.*, 1975, **8**, 300; (*b*) J. B. Lambert and S. I. Featherman, *Chem. Rev.*, 1975, **75**, 611; (*c*) T. A. Crabb and A. R. Katritzky, *Adv. Heter. Chem.*, 1984, **36**, 1; (*d*) for a condensed discussion, see S. Profeta and N. L. Allinger, *J. Am. Chem. Soc.*, 1985, **107**, 1907; (*e*) J. B. Lambert and Y. Takeuchi, *Acyclic Organonitrogen Stereodynamics*, VCH, New York, 1992; (*f*) J. B. Lambert and Y. Takeuchi, *Cyclic Organonitrogen Stereodynamics*, VCH, New York, 1992.

2 J. H. Brown and C. H. Bushweller, *J. Am. Chem. Soc.*, 1992, **114**, 8153; J. E. Anderson, D. Casarini and L. Lunazzi, *J. Chem. Soc., Perkin Trans. 2*, 1990, 1791.

3 D. A. Forsyth, W. Zhang and J. A. Hanley, *J. Org. Chem.*, 1996, **61**, 1284; C. H. Bushweller, J. H. Brown, C. M. DiMeglio, G. W. Gribble, J. T. Eaton, C. S. LeHoullier and E. R. Olson, *J. Org. Chem.*, 1995, **60**, 268; S. F. Nelsen, J. T. Ippoliti, T. B. Frigo and P. A. Petillo, *J. Am. Chem. Soc.*, 1989, **111**, 1776.

4 In cyclohexane the transition state connecting the chair and twist-boat conformations was found to be of C_2 and C_1 geometry: D. A. Dixon and A. Komornicki, *J. Phys. Chem.*, 1990, **94**, 5630.

5 (*a*) N. Kolocouris, A. Kolocouris, G. B. Foscolos, G. Fytas, J. Neyts, E. Padalko, J. Balzarini, R. Snoeck, G. Andrei and E. De Clercq, *J. Med. Chem.*, 1996, **39**, 3307; (*b*) N. Kolocouris, G. B. Foscolos, A. Kolocouris, P. Marakos, N. Pouli, G. Fytas, S. Ikeda and E. De Clercq, *J. Med. Chem.*, 1994, **37**, 2896; (*c*) A. Kolocouris, Ph.D. Thesis, University of Athens, 1995.

6 G. Fytas, G. Stamatiou, G. B. Foscolos, A. Kolocouris, N. Kolocouris, M. Witvrouw, C. Pannecouque and E. De Clercq, *Biorg. Med. Chem. Lett.*, 1997, 1887.

7 C. L. Perrin and T. J. Dwyer, *Chem. Rev.*, 1990, **90**, 935.

8 For ^{1}H NMR spectroscopy of adamantane derivatives, see (*a*) R. C. Fort and P. v. R. Schleyer, *J. Org. Chem.* 1965, **30**, 789; (*b*) F. W. van Deursen and P. K. Korver, *Tetrahedron Lett.*, 1967, 3923; (*c*) F. W. van Deursen and A. C. Udding, *Recl. Trav. Chim. Pays-Bas*, 1968, **87**, 1243; (*d*) F. W. van Deursen and J. Bakker, *Tetrahedron*, 1971, 4593; (*e*) D. Hofner, S. A. Lesko and G. Binsch, *Org. Magn. Res.*, 1978, **11**, 79; (*f*) R. J. Abraham and J. Fisher, *Magn. Reson. Chem.*, 1985, **23**, 856; (*g*) R. J. Abraham and J. Fisher, *Magn. Reson. Chem.*, 1985, **23**, 866.

9 For ^{13}C NMR spectroscopy of adamantane derivatives, see (*a*) T. Pehk, E. Lippmaa, V. V. Sevostjanova, M. Krayuschkin and A. I. Tarasova, *Org. Magn. Reson.*, 1971, **3**, 783; (*b*) G. E. Maciel, H. C. Dorn, R. L. Greene, W. A. Kleschick, M. R. Peterson and G. H. Wahl, *Org. Magn. Reson.*, 1974, **6**, 178; (*c*) H. Duddeck and W. Dietrich, *Tetrahedron Lett.*, 1975, 2925; (*d*) H. Duddeck, *Org. Magn. Reson.*, 1975, 171; (*e*) H. Duddeck and P. Wolff, *Org. Magn. Reson.*, 1976, **8**, 593; (*f*) H. Duddeck, F. Hollowood, A. Karim and M. A. McKervey, *J. Chem. Soc., Perkin Trans. 2*, 1979, 360; (*g*) H. Duddeck and Md. R. Islam, *Org. Magn. Reson.*, 1981, **16**, 32; (h) D. M. Doddrell, D. T. Pegg and M. R. Bendall, *J. Magn. Reson.*, 1982, **48**, 323; (*i*) M. R. Bendall and D. T. Pegg, *J. Magn. Reson.*, 1983, **53**, 272; (*j*) J. S. Lomas, C. Cordier, S. Briand and J. Vaissermann, *J. Chem. Soc., Perkin Trans. 2*, 1996, 871.

10 For the straightforward assignment of the ^{13}C NMR chemical shifts of some 1- and 2- substituted and 2,2-disubstituted adamantanes, see V. V. Krishnamurthy, P. S. Iyer and G. A. Olah. *J. Org. Chem.*, 1983, **48**, 3373.

11 A. J. Jones, C. P. Beeman, M. U. Hasan, A. F. Casy and M. M. A. Hassan, *Can. J. Chem.*, 1976, **54**, 126.

12 The orientation of the 4′, 9′ and 8′, 10′ protons is referred to the 1′-2′-3′-4′-5′-9′ and 1′-2′-3′-10′-7′-8′ adamantane rings, respectively, as has been described in ref. 8*b*.

13 (*a*) F. A. L. Anet and M. Kopelvich, *J. Am. Chem. Soc.*, 1986, **108**, 2109; (*b*) F. W. Vierhapper and E. L. Eliel, *J. Org. Chem.*, 1975, **40**, 2734; (*c*) E. L. Eliel, F. W. Vierhapper and G. Z. Juaristi, *Tetrahedron Lett.*, 1975, 4339.

14 E. L. Eliel and K. M. Pietrusiewicz, *Top. C-13 NMR Spectrosc.*, 1979, **3**, 171.

15 E. L. Eliel, W. F. Bailey, L. D. Kopp, R. L. Willer, D. M. Grant, R. Bertrand, K. A. Christensen, D. K. Dalling, M. W. Duch, E. Wenkert, F. M. Schell and D. W. Cochran, *J. Am. Chem. Soc.*, 1975, **97**, 322 and references therein.

16 For similar shifts, see E. L. Eliel and F. W. Vierhapper, *J. Org. Chem.*, 1976, **41**, 199; E. L. Eliel, D. Kandasamy, C.-Y. Yen and K. D. Hargrave, *J. Am. Chem. Soc.*, 1980, **102**, 3698.

17 For a discussion related to the interconversion barriers of many simple nitrogen heterocycles, see A. R. Katritzky, R. C. Patel and F. G. Ridell, *Angew. Chem., Int. Ed. Engl.*, 1981, **20**, 521.

18 F. A. L. Anet, I. Yavari, I. J. Ferguson, A. R. Katritzky, M. Moreno-Manas and M. J. T. Robinson, *J. Chem. Soc., Chem. Commun.*, 1976, 399.

19 R. W. Alder, E. Heilbroner, E. Honegger, A. B. McEwen, R. E. Moss, E. Olefirowicz, P. A. Petillo, R. B. Sessions, G. R. Weisman, J. M. White and Z.-Z. Yang, *J. Am. Chem. Soc.*, 1993, **115**, 6580.

20 (*a*) F. Mohamadi, N. G. J. Richards, W. C. Guida, R. Liskamp, M. Lipton, C. Caufield, G. Chang, T. Hendrickson and W. C. Still, *J. Comput. Chem.*, 1990, **11**, 440; the Monte Carlo method implemented in the Macromodel software is described in detail in G. Chang, W.C. Guida and W. C. Still, *J. Am. Chem. Soc.*, 1989, **111**, 4379 and M. Saunders, K. N. Houk, Y.-D. Wu, W. C. Still, M. Lipton, G. Chang and W. C. Guida, *J. Am. Chem. Soc.*, 1990, **112**, 1419; (*b*) Hyperchem is developed and licenced from Hypercube Inc. The MM+ force field used in this software for molecular mechanics calculations is an extension of MM2 (N. L. Allinger, *J. Am. Chem. Soc.*, 1977, **99**, 8127, using the MM2 (1991) parameters and atom types with the 1977 functional form.

Paper 7/05868C
Received 11*th August* 1997
Accepted 27*th March* 1998